Hindawi
Journal of Chemistry
Volume 2020, Article ID 4106562, 11 pages
https://doi.org/10.1155/2020/4106562

Research Article

Theoretical Investigation on Structure-Property Relationship of Asymmetric Clusters $(CH_3FBN_3)_n$ $(n = 1–6)$

Deng-Xue Ma,[1] Yao-Yao Wei,[2] Yun-Zhi Li,[2] Guo-Kui Liu,[2] and Qi-Ying Xia[2]

[1]*School of Materials Science and Engineering, Linyi University, Linyi 276005, China*
[2]*School of Chemistry and Chemical Engineering, Linyi University, Linyi 276005, China*

Correspondence should be addressed to Guo-Kui Liu; liuguokuihappy@163.com and Qi-Ying Xia; xiaqiying@163.com

Received 2 April 2020; Revised 15 May 2020; Accepted 11 June 2020; Published 30 June 2020

Academic Editor: Franck Rabilloud

The structural, relative stability, electronic, IR vibrational, and thermodynamic properties of asymmetric clusters $(CH_3FBN_3)_n$ $(n = 1–6)$ are systematically investigated using density functional theory (DFT) method. Results show that clusters $(CH_3FBN_3)_n$ $(n = 2–6)$ form a cyclic structure with a B atom and a N_α atom binding together. Five main characteristic regions are observed and assigned for the calculated IR spectra. The size-dependent second-order energy difference shows that clusters $(CH_3FBN_3)_3$ and $(CH_3FBN_3)_5$ have relatively higher stability and enhanced chemical inertness compared with the neighboring clusters. These two clusters may serve as the cluster-assembled materials. The variations of thermodynamic properties with temperature T or cluster size n are analyzed, respectively. Based on enthalpies in the range of 200–800 K, the formations of the most stable clusters $(CH_3FBN_3)_n$ $(n = 2–6)$ from monomer are thermodynamically favorable. These data are helpful to design and synthesize other asymmetric boron azides.

1. Introduction

The extensive studies on boron azides are developed as these molecules have been shown to be good precursors for boron nitride (BN) film deposition [1]. The chemistry of boron azides commenced in 1954 with the synthesis of boron triazide $B(N_3)_3$ [2]; since then, it developed slowly. In 1963, Paetzold produced trimeric $(Cl_2BN_3)_3$ from the reaction of LiN_3 and BCl_3 in CH_2Cl_2 solution [3]. The molecular structure of dichloroboron azide containing six-membered boron nitrogen heterocycle with diazo groups bounded to nitrogen atoms was determined by Müller in 1971 [4]. Boron dihalide azides $(BX_2N_3)_3$ (X = F, Cl, or Br) from the reaction of BCl_3 with trimethylsilyl azide in CH_2Cl_2 solution were also recorded by Wiberg et al. in 1972 [5]. Dehnicke reported the infrared spectra of the monoazide products, I_2MN_3 (M = B, Al, Ga), and observed the formation of oligomers of these species in 1978 [6]. Several alkyl and arylboron azides have been synthesized using similar methods. Oligomerization for Me_2BN_3 was established by ^{11}B NMR spectroscopy in 1966 [7]. The chemistry of alkylboron azides was further investigated, and the development of this field has been reviewed by Paetzold, Fraenk, and coworkers [8–16].

Although the chemistry of boron azides in the condensed phase has been extensively discussed in the literature, research studies of these species in the gas phase are rather limited. With the goal to use boron azides as the single-source precursors (SSP), knowledge of their gas phase stability and thermodynamic properties becomes essential. The structure of monomers Cl_2BN_3 and $(CH_3)_2BN_3$ has been explored using ab initio calculation, and the thermodynamic stabilities of X_2BN_3 with respect to its dimerization and trimerization have been gained and discussed [17–20] from the theoretical view. Previous theoretical studies of the boron azides mostly focused on the symmetric boron azides.

The effect for the break of the symmetry of substituted boron azides is hardly considered. Here, in accordance with previous theoretical studies on the asymmetric clusters of inorganic boron azides [21, 22], and experimental studies on the asymmetric clusters of organic gallane azides and aluminum azides $(RR'MN_3)_n$ (M = Al, Ga; R = CH_3; R' = H, Cl, Br; n = 3–4) [23, 24], the structure, stability, IR spectra, and

thermodynamic characteristics of the asymmetric clusters of organic boron azides $(CH_3FBN_3)_n$ $(n = 1 - 6)$ were theoretically discussed in detail. These discussions will provide fundamental data and references for experimentalist to design and synthesize the novel boron azides in the future.

2. Computational Methods

As is well known, it is important to choose an appropriate basis set to give the accurate description of clusters' structures and energies. Usually, a substantial size of basis set is required. However, the size of clusters studied in this work excluded the use of a very large basis set, and hence, all calculations were performed using the DFT-B3LYP method with the 6-31G* basis set [25, 26] via the Gaussian 09 program package with the default convergence thresholds [27]. To ensure the adequacy of this basis set, we also optimized the clusters with the 6-311 + G* basis set. As shown later on, results obtained from these two basis sets were similar except for slightly numerical differences. The energies of all clusters were also evaluated using the 6-311 + G* basis set. The initial configurations are searched by two ways: (1) by considering the numbers of known clusters $(HClBN_3)_n$ $(n = 1–6)$ in previous works [21] and (2) by placing -CH_3 groups and F atoms at various substitutional sites (H or Cl) on the basis of optimized $(HClBN_3)$ geometries. No symmetry constraints were applied. Lots of rationally initial one-, two-, and three-dimensional configurations were built to seek the most stable structures. In this way, a large number of optimized isomers for the asymmetric clusters $(CH_3FBN_3)_n$ $(n = 1–6)$ were obtained. Frequencies as well as their respective IR intensities were then calculated, and the lack of imaginary frequencies confirmed that the true minimum was obtained in each case. According to the previous study, the calculated frequencies were scaled uniformly by 0.96 to approximately correct the systematic overestimation [28].

3. Results and Discussion

3.1. Structures and Charge Distribution. A number of isomers are calculated at each size. Here, structures of clusters $(CH_3FBN_3)_n$ $(n = 1 - 6)$ having the lowest energy were focused because all properties of clusters $(CH_3FBN_3)_n$ $(n = 1–6)$ were calculated based on the lowest energy. Two stable structures of the monomer CH_3FBN_3 were obtained (connectivity: $CH_3FB–N_\alpha–N_\beta–N_\gamma$) with a slight difference in geometrical parameters. The clusters $(CH_3FBN_3)_n$ $(n = 2 - 6)$ are produced by the head-to-tail oligomerization of the CH_3FBN_3 monomers, which is a starting point for the oligomerizations. Two dimers, seventeen trimers, sixty-four tetramers, two hundred and fifty-six pentamers, and five hundred and thirty-six hexamers are obtained in this manner. Judged by the total energies, the most stable isomers at each size are labeled as 1, 2, 3, 4, 5, and 6 and shown in Figure 1. Obviously, B and N_α atoms easily bond together, and B–B and $N_\alpha–N_\alpha$ bonds are not formed in the clusters $(CH_3FBN_3)_n$ $(n = 2 - 6)$. In other words, the clusters $(CH_3FBN_3)_n$ $(n = 2 - 6)$ contain cyclic $(BN_\alpha)_{2n}$ structures with alternating boron and α-nitrogen atoms.

The corresponding geometrical parameters are collected in Table 1, and the data in parentheses are calculated results from the 6-311 + G* basis set. The results obtained from different basis sets are generally consistent. In detail, bond lengths (except for B–F bonds) from the 6-311 + G* basis set are slightly shorter than those from the 6-31G* basis set. This whole agreement shows that it is appropriate to choose the 6-31G* basis set to compute the titled systems. Therefore, in this work, we only report the geometrical parameters obtained with the 6-31G* basis set. For $n = 1$, the azide group in the monomer CH_3FBN_3 is slightly bent with a $N_\alpha–N_\beta–N_\gamma$ angle of 173.1°. The calculated B–N bond length of 1.447 Å is between B–N single (1.58 Å) and double bonds (1.37 Å). The $N_\beta–N_\gamma$ bond length at 1.135 Å is shorter than the $N_\alpha–N_\beta$ bond length at 1.240 Å. The $N_\beta–N_\gamma$ bond length is between N–N double (1.25 Å) and N–N triple bonds (1.10 Å). For $n = 2 - 6$, the computed B–N bond length of 1.601–1.638 Å possesses typical character of B–N single bond, which is similar to the B–N length of other covalent boron azides previously determined, such as $(F_2BN_3)_3$ (1.616 Å) [19] and $(C_6F_5B(N_3)_2)_3$ (1.60 Å) [12]. The B–C and B–F bond lengths are in the range of 1.585–1.596 Å and 1.363–1.381 Å, respectively. The computed structural parameters of the azide units in the clusters $(CH_3FBN_3)_n$ $(n = 2 - 6)$ are 1.240–1.255 Å for $N_\alpha–N_\beta$ bonds, 1.128–1.133 Å for $N_\beta–N_\gamma$ bonds, and 177.1–179.4° for $N_\alpha–N_\beta–N_\gamma$ bond angle. It is obvious that the azide group is nearly linear. These results are perfectly consistent with those found in $(Cl_2BN_3)_3$ (1.25 Å, 1.09 Å, 178°) [4], $(F_2BN_3)_3$ (1.249 Å, 1.129 Å, 179.8°) [19], and $(C_6F_5B(N_3)_2)_3$ (1.27 Å, 1.11 Å, 179°) [12]. Therefore, the calculation method in this work is reliable, and it gives credence to our computed structural parameters of clusters $(CH_3FBN_3)_n$ $(n = 2 - 6)$.

Through the above discussions, it is obvious that $N_\beta–N_\gamma$ bond is shorter than $N_\alpha–N_\beta$ bond in the clusters $(CH_3FBN_3)_n$ $(n = 1 - 6)$. This can be interpreted as a higher bond order for the terminal N–N bond, showing a preformation of the N_2 molecule. Moreover, the cluster size n has an important effect on the geometries. An obvious increase is shown for the length of B-N_α bond with cluster size n increasing from 1 to 2~6 owing to the tension of the ring. However, B–N_α bond length shows little change with cluster size in the range of 2~6, which fluctuates in the range of 1.601–1.638 Å. The $N_\alpha–N_\beta$ bond lengths increase as the cluster size n increases from 1 to 5 and show little change from $n = 5$ to $n = 6$. Similarly, when cluster size n increases from 1 to 3, the B–C and B–F bond lengths increase. However, the change of B–C and B–F bond lengths is not obvious from $n = 4$ to $n = 6$. The $N_\beta–N_\gamma$ bond length shortens from 1.135 Å in cluster size with 1 to 1.129 Å in cluster size with 6 and tends to be constant around 1.130 Å with $n = 3 - 6$. Compared with monomer 1, the increasing bond lengths of $N_\alpha–N_\beta$, B–C and B–F bonds that are outside of rings show that N_2 ($N_\beta–N_\gamma$), -CH_3, and F^- groups can be easily removed to yield BN material.

To give a deeper understanding on these structures, we calculate the charge distribution of the clusters $(CH_3FBN_3)_n$ $(n = 1 - 6)$ as shown in Table 2. It can be seen that the charge distribution of CH_3FBN_3 molecule exhibits zwitterionic

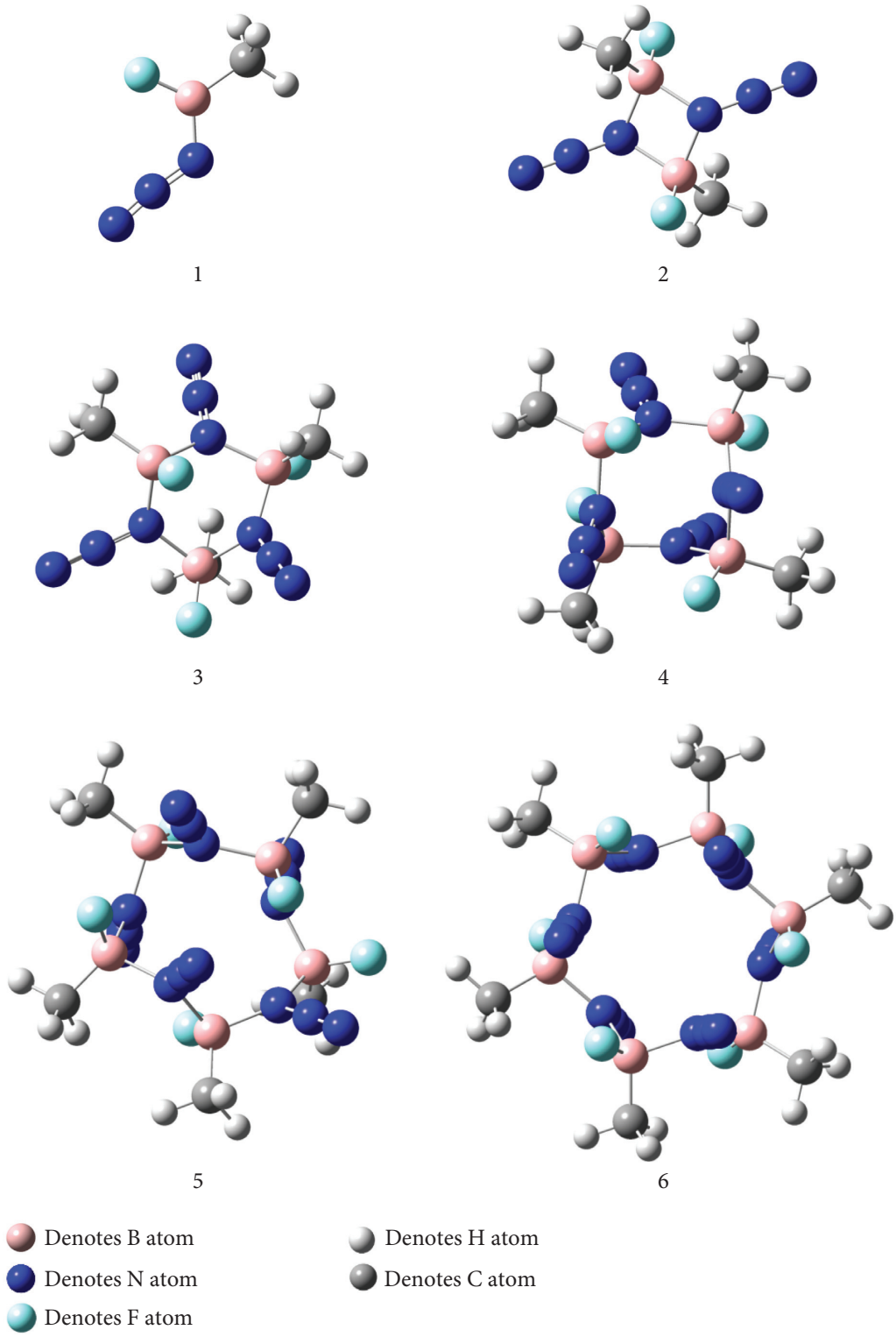

Figure 1: Structures of the asymmetric clusters $(CH_3FBN_3)_n$ $(n = 1–6)$.

characteristics with the charge centers of N and B atoms, respectively. As for $(CH_3FBN_3)_n$ $(n = 2 – 6)$, charge distributions are similar to those of CH_3FBN_3. However, because B atoms in these molecules all reach the high coordination, the characteristic of zwitterionic ion for these clusters is a problem needing more studies.

3.2. Relative Stabilities. All energies are displayed in Table 3, and the data in parentheses are from the 6-311 + G* basis set. Obviously, the energies obtained at the B3LYP/6-31G* levels are similar to those obtained with the 6-311 + G* basis set. The use of larger basis sets has no significant influence on the binding energies, which again shows that the 6-31G* basis

Table 1: Ranges of the bond lengths (Å) and bond angles (deg) for the most stable structures of the asymmetric clusters (CH_3FBN_3) (n) $(n = 1 – 6)$ optimized at the DFT-B3LYP level[a].

	1	2	3	4	5	6
N_β–N_γ	1.135 (1.126)	1.133 (1.125)	1.128–1.133 (1.120–1.125)	1.133 (1.121)	1.128–1.133 (1.119–1.124)	1.129 (1.120)
N_α–N_β	1.240 (1.236)	1.240 (1.235)	1.243–1.246 (1.240–1.249)	1.248 (1.246)	1.246–1.255 (1.243–1.253)	1.251 (1.250)
N_α–B	1.447 (1.442)	1.633 (1.641–1.643)	1.614–1.638 (1.613–1.632)	1.601–1.602 (1.598–1.600)	1.608–1.637 (1.603–1.627)	1.606 (1.601–1.604)
B–C	1.563 (1.555)	1.585 (1.579)	1.589–1.593 (1.584–1.588)	1.591 (1.587)	1.591–1.596 (1.587–1.591)	1.592 (1.588)
B–F	1.341 (1.349)	1.363 (1.374)	1.376–1.381 (1.388–1.393)	1.385 (1.397)	1.380–1.386 (1.387–1.398)	1.387–1.388 (1.398–1.399)
C–H	1.093–1.098 (1.091–1.096)	1.096–1.098 (1.094–1.096)	1.094–1.098 (1.092–1.096)	1.096–1.098 (1.094–1.096)	1.093–1.098 (1.091–1.096)	1.094–1.098 (1.093–1.096)
B–N_α–B		94.1 (95.2)	124.7–125.2 (123.9–125.0)	126.7–126.9 (127.1)	126.3–128.2 (125.6–131.2)	125.2–125.3 (126.0–126.1)
N_α–B–N_α		85.9 (84.8)	100.2–100.7 (99.3–100.7)	102.9–103.1 (103.3)	105.0–107.8 (104.1–106.4)	106.2–106.2 (106.6–106.7)
N_α–N_β–B	121.3 (121.4)	123.3.1–124.6 (125.6–125.8)	117.6–119.6 (115.6–119.4)	114.9–118.4 (118.0–118.6)	115.5–118.7 (113.3–118.0)	118.2–118.4 (117.4–117.5)
N_α–N_β–N_γ	173.1 (173.3)	177.1 (177.5)	177.8–178.9 (178.1–179.1)	178.3–178.4 (178.3–178.4)	178.2–179.4 (178.3–179.4)	177.6–177.8 (177.6–177.9)

[a]The data in parentheses are from 6-311 + G* basis set.

Table 2: Atomic charge (e) of the most stable structure $(CH_3FBN_3)_n$ $(n = 1 – 6)$.

	1	2	3	4	5	6
N_α	−0.5840	−0.5922	−0.5847	−0.5885	−0.5854	−0.5918
N_β	0.2447	0.2761	0.2760	0.2753	0.2704	0.2686
N_γ	−0.0175	0.0299	0.0512	0.0602	0.0608	0.0673
B	1.1319	1.0869	1.0721	1.0745	1.0773	1.0809
F	−0.4760	−0.4973	−0.5100	−0.5174	−0.5171	−0.5227
C	−1.0830	−1.0571	−1.0545	−1.0551	−1.0568	−1.0561
H	0.2627	0.2512	0.2499	0.2504	0.2503	0.2503

Table 3: Total energies (E), zero point energy (ZPE), uncorrected binding energies (E_b), corrected binding energies ($E_{b\text{-}c}$), average corrected binding energy ($E_{b\text{-}c\text{-ave}}$), and second-order energy difference ($\Delta_2 E$) (unit: $kJ \cdot mol^{-1}$)[a].

Clusters	E	E_b	ZPE	$E_{b\text{-}c}$	$E_{b\text{-}c\text{-ave}}$	$\Delta_2 E$
1	−863544.11 (−863796.61)		150.49 (149.36)			
2	−1727098.45 (−1727602.68)	10.23 (9.45)	306.95 (304.09)	4.50 (4.30)	2.25 (2.15)	−29.27 (−27.67)
3	−2590684.89 (−2591439.62)	52.56 (49.78)	466.36 (462.16)	38.27 (36.26)	12.76 (12.09)	18.76 (16.97)
4	−3454250.88 (−3455257.97)	74.44 (71.51)	624.01 (618.54)	53.27 (51.26)	13.32 (12.81)	−3.75 (−4.25)
5	−4317819.67 (−4319078.66)	99.12 (95.59)	780.67 (772.93)	72.03 (70.51)	14.41 (14.10)	3.97 (5.01)
6	−5181384.41 (−5182894.97)	119.75 (115.28)	937.24 (927.98)	86.82 (84.74)	14.47 (14.12)	

[a]The data in parentheses are from 6-311 + G* basis set.

set is suitable for the clusters studied here. Thus, in this work, we only report the relative stability of the clusters $(CH_3FBN_3)_n$ with the 6-31G* basis set. The uncorrected binding energies (E_b), corrected binding energies ($E_{b\text{-}c}$), average corrected binding energy ($E_{b\text{-}c\text{-ave}}$), and the second-order energy difference ($\Delta_2 E$) are calculated using the following equations:

$$
\begin{aligned}
E_{\mathrm{b}}(n) &= nE\left(\mathrm{CH_3FBN_3}\right) - E\left(\mathrm{CH_3FBN_3}\right)_n,\\
E_{b-c}(n) &= nE\left(\mathrm{CH_3FBN_3}\right) + 0.96 * nZPE\left(\mathrm{CH_3FBN_3}\right) - E\left(\mathrm{CH_3FBN_3}\right)_n - 0.96 * ZPE\left(\mathrm{CH_3FBN_3}\right)_n,\\
E_{b-c-\mathrm{ave}}(n) &= \frac{E_{b-c}(n)}{n},\\
\Delta_2 E(n) &= E\left(\mathrm{CH_3FBN_3}\right)_{n+1} + 0.96 * ZPE\left(\mathrm{CH_3FBN_3}\right)_{n+1} + E\left(\mathrm{CH_3FBN_3}\right)_{n-1}\\
&\quad + 0.96 * ZPE\left(\mathrm{CH_3FBN_3}\right)_{n-1} - 2E\left(\mathrm{CH_3FBN_3}\right)_n - 2 * 0.96 * ZPE\left(\mathrm{CH_3FBN_3}\right)_n,
\end{aligned}
\tag{1}
$$

where $E\left(\mathrm{CH_3FBN_3}\right)_n$ and $E\left(\mathrm{CH_3FBN_3}\right)$ are the total energies of the clusters $\left(\mathrm{CH_3FBN_3}\right)_n$ ($n = 2-6$) and $\mathrm{CH_3FBN_3}$, respectively; $ZPE\left(\mathrm{CH_3FBN_3}\right)_n$ and $ZPE\left(\mathrm{CH_3FBN_3}\right)$ represent the zero point energies of the most stable clusters $\left(\mathrm{CH_3FBN_3}\right)_n$ ($n = 2-6$) and $\mathrm{CH_3FBN_3}$, respectively; and the 0.96 is a scaling factor [28].

From Table 3, the ratios of *ZPE* corrections to their binding energies E_b are large for the clusters $\left(\mathrm{CH_3FBN_3}\right)_n$ ($n = 2-6$). Thus, it is necessary to carry out the *ZPE* corrections for the binding energies. For intuitive presentation, the calculated energy is also plotted as a function of cluster size n as shown in Figure 2. The curves of E_b (Figure 2(a)) and $E_{b\text{-}c}$ (Figure 2(b)) are seen to increase monotonically with the augment of cluster size n, which means that clusters can continue to gain energy during the clusters' growth process. The $E_{b\text{-}c\text{-ave}}$ values increase sharply with the clusters size n from 2 to 3; then, it approaches to be stable around 13–14 kJ·mol^{-1} when cluster size $n \geq 3$. Therefore, the geometrical structures of clusters $\left(\mathrm{CH_3FBN_3}\right)_n$ ($n = 1-6$) tend to be stable when cluster size $n \geq 3$.

The relative stability of clusters can be also estimated through the $\Delta_2 E$ (n). According to the definition, clusters with positive $\Delta_2 E$ are more stable than those with negative $\Delta_2 E$. A clear odd-even oscillation behavior is presented in Figure 2(d). The clusters $\left(\mathrm{CH_3FBN_3}\right)_n$ ($n = 1-6$) at $n = 3$, 5 correspond to local maximal on the curve of $\Delta_2 E$, indicating that they are relatively more stable than other clusters. This trend is in excellent agreement with that of the asymmetric clusters of the inorganic boron azides $\left(\mathrm{HClBN_3}\right)_n$ ($n = 1-6$) [21]. In particular, the trimer $\left(\mathrm{CH_3FBN_3}\right)_3$ possesses the highest stability among all clusters in terms of the largest value of $\Delta_2 E$. The stable structure of six-member ring of trimer plays a vital role.

3.3. IR Spectrum. The IR spectrum is not only the basic property of compounds and effective method to analyze or identify substances, but also has a direct relationship with thermodynamic properties. However, there are no experimental data for the title compounds. Thus, it is necessary to use the theoretical method to calculate and predict IR spectra for both theoretical and practical reasons. Figure 3 provides the calculated IR spectra of the clusters $\left(\mathrm{CH_3FBN_3}\right)_n$ ($n = 1-6$) at the B3LYP/6-31G* level. Due to intrinsic complexity, it is difficult to assign all vibrational modes. Thus, we only analyze and discuss some typical vibrational modes.

There are five main characteristic regions for clusters $\left(\mathrm{CH_3FBN_3}\right)_n$ ($n = 1-6$) that correspond to the $-N_3$ asymmetric and symmetric stretching, $-CH_3$ stretching and in-plane bending vibrations, and the fingerprint region. As for monomer $\mathrm{CH_3FBN_3}$, the $-N_3$ asymmetric and symmetric stretching vibrations with intense peak lie at 2215 and 1360 cm^{-1}, respectively. The modes in the range of 2923–3022 cm^{-1} are classified to the characteristic $-CH_3$ stretching vibrations. The peak around 1440 cm^{-1} corresponds to the $-CH_3$ in-plane bending vibrations. The peaks at less than 1210 cm^{-1} belong to the fingerprint region, which are mainly composed of wagging and scissoring of $-CH_3$ and the stretching of B–F and B–C bonds. As can be seen from Figure 3, similar vibrational modes are observed in clusters $\left(\mathrm{CH_3FBN_3}\right)_n$ ($n = 2-6$). The regions of 2917–3019, 2202–2243, 1331–1458, 1217–1308, and 0–1204 cm^{-1} are individually assigned to $-CH_3$ stretching vibrations, $-N_3$ asymmetric stretching vibrations, $-CH_3$ in-plane bending vibrations, $-N_3$ symmetric stretching vibrations, and fingerprint region. In previous studies, the N–N asymmetrical stretching vibration for Cl_2BN_3, Br_2BN_3, Me_2BN_3, $(C_6F_5)_2BN_3$ polymer, and NaN_3 crystal were individually located at 2210–2219 [15], 2200–2215 [15], 2128 [7, 14], 2135–2209 cm^{-1} [11, 12], and 2128–2151 cm^{-1} [29] from experiments. Our calculated results are in accordance with those in crystal, which shows that the structures of N_3 groups in clusters and in crystal are identical. Moreover, the obtained result is similar to that found in the clusters $\left(\mathrm{HClBN_3}\right)_n$ ($n = 1-6$) (2217–2250 cm^{-1}) of DFT calculations [21].

Furthermore, compared with monomer, the N_3 asymmetric stretching vibration presents the blue-shifted phenomenon for clusters with $n = 2-6$. However, the N_3 symmetric stretching vibration and the $-CH_3$ stretching vibration show red-shifted trend. Meanwhile, in three characteristic regions of N_3 asymmetric, N_3 symmetric, and $-CH_3$ stretching vibration, the number of vibration mode equals to that of azido groups and C–H bonds, respectively. For example, the monomer 1 has three bands at 2923, 2972, and 3022 cm^{-1} with C–H stretching vibration, and the trimer 3 has three bands at 2213, 2225, and 2240 cm^{-1} with N_3 asymmetric stretching vibration, and the hexamer 6 has six bands at 1237, 1237, 1245, 1245, 1247, and 1255 cm^{-1} with N_3 symmetric stretching vibration.

3.4. Thermodynamic Properties. Thermodynamic functions are important parameters for clusters to predict reactive

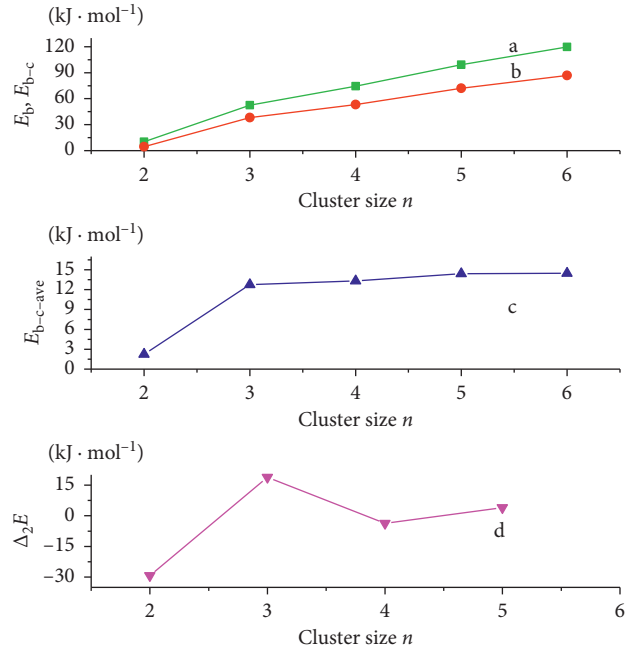

FIGURE 2: The uncorrected binding energies E_b (a), corrected binding energies $E_{b\text{-}c}$ (b), average corrected binding energy $E_{b\text{-}c\text{-ave}}$ (c), and the second-order energy difference $\Delta_2 E$ (d) of the asymmetric clusters $(CH_3FBN_3)_n$ $(n = 1-6)$ versus the cluster size n.

property in a chemical reaction. According to vibrational analysis and statistical thermodynamic method, the standard molar heat capacity ($C^\theta_{p,m}$), standard molar thermal entropy (S^θ_m), and standard molar thermal enthalpy (H^θ_m) of the asymmetric clusters $(CH_3FBN_3)_n$ $(n = 1-6)$ in the range of 200–800 K are evaluated and tabulated in Table 4. It is obvious that the calculated thermodynamic functions increase with the temperature T raising. For more clear intuitive, taking monomer 1 as an example, the temperature-dependent relationships for $C^\theta_{p,m}$, S^θ_m, and H^θ_m are expressed in formulas (2)–(4) and all are plotted in Figure 4(a). These correlations approximate to linear equations due to the small coefficients of T^2; namely, the $C^\theta_{p,m}$, S^θ_m, and H^θ_m increase linearly with the increase of temperature T. This can be understood from the fact that these three thermodynamic functions are dominated by the weak translational and rotational motions of the clusters at lower temperature, whereas the vibrational motion is intensified and makes more contributions to $C^\theta_{p,m}$, S^θ_m, and H^θ_m at higher temperature. The same linear relationships are found for clusters $(CH_3FBN_3)_n$ with $n = 2-6$:

$$\begin{aligned} C^\theta_{p,m} &= 33.4650 + 0.2460\,T - 1.1698 \times 10^{-4} T_2, \\ R^2 &= 0.9999, \\ \mathrm{SD} &= 0.3318, \end{aligned} \tag{2}$$

$$\begin{aligned} S^\theta_m &= 231.0291 + 0.4049\,T - 1.4317 \times 10^{-4} T^2, \\ R^2 &= 0.9998, \\ \mathrm{SD} &= 0.9034, \end{aligned} \tag{3}$$

$$\begin{aligned} H^\theta_m &= -3.6904 + 0.0606\,T + 6.401 \times 10^{-5} T^2, \\ R^2 &= 0.9999, \\ \mathrm{SD} &= 0.2784, \end{aligned} \tag{4}$$

where R^2 represents the square of correlation coefficient and SD represents standard deviation.

Moreover, the cluster size-dependent relationships for $C^\theta_{p,m}$, S^θ_m, and H^θ_m are expressed in formulas (5)–(7) and all are shown in Figure 4(b). All thermodynamic functions increase monotonically with the enlarged cluster size n; in other words, when one more CH_3FBN_3 is bound, the $C^\theta_{p,m}$, S^θ_m, and H^θ_m increase with the average of 108 J·mol^{-1} K^{-1}, 133 J·mol^{-1} K^{-1}, and 18 kJ·mol^{-1}, separately. This means that the contribution of monomer CH_3FBN_3 to the thermodynamic properties of cluster matches the cluster additivity:

$$\begin{aligned} C^\theta_{p,m} &= -12.0847 + 108.4637\,n, \\ R^2 &= 1.0000, \\ \mathrm{SD} &= 1.0282, \end{aligned} \tag{5}$$

$$\begin{aligned} S^\theta_m &= 211.0987 + 133.2237\,n, \\ R^2 &= 0.9996, \\ \mathrm{SD} &= 8.0272, \end{aligned} \tag{6}$$

$$\begin{aligned} H^\theta_m &= 1.0620 + 18.3966\,n, \\ R^2 &= 0.9999, \\ \mathrm{SD} &= 0.5260. \end{aligned} \tag{7}$$

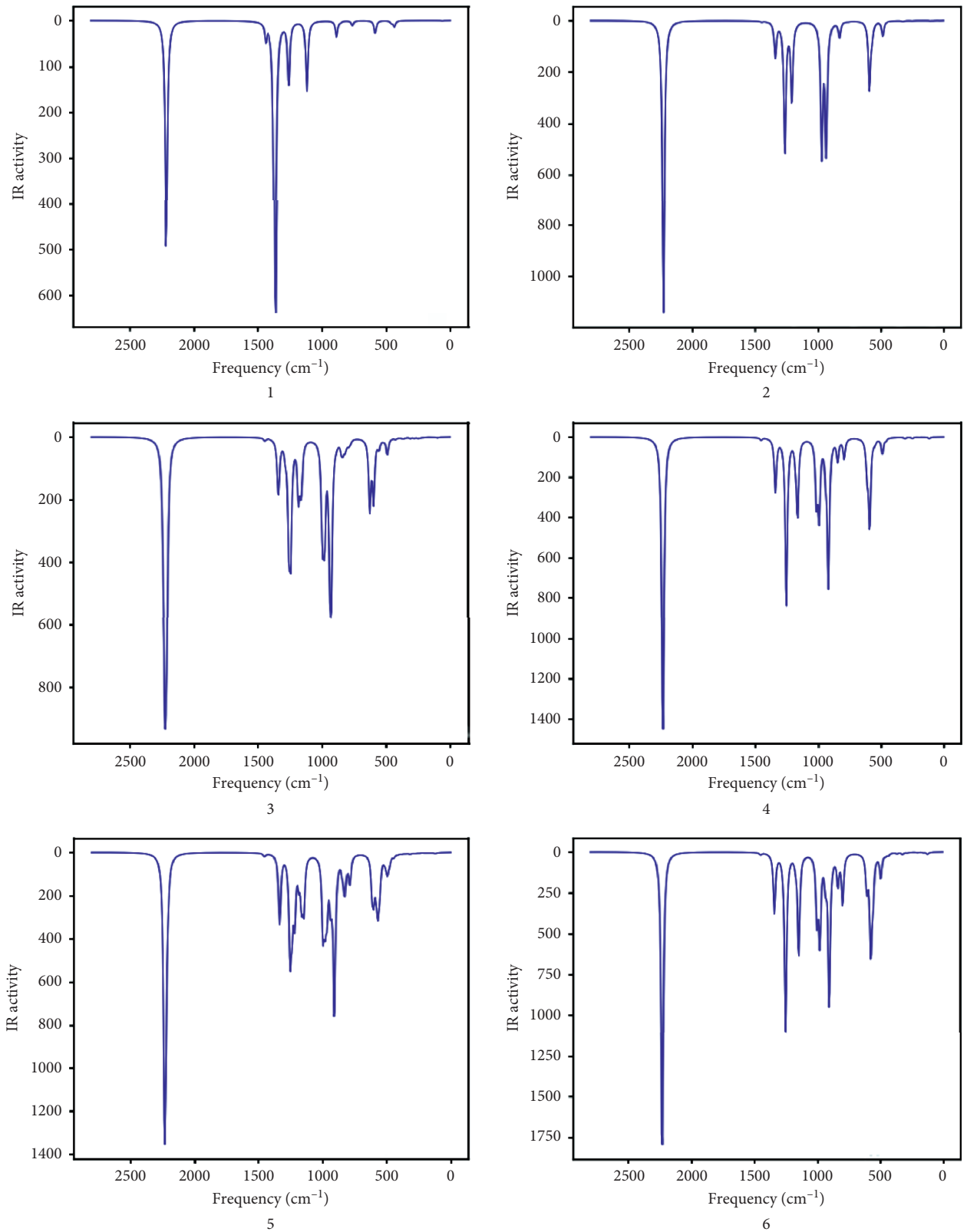

Figure 3: IR spectra of the asymmetric clusters $(CH_3FBN_3)_n$ $(n = 1 - 6)$ with full width at half maxima of 20 cm^{-1}.

In addition, the theoretical enthalpies (ΔH) and Gibbs free energies (ΔG) of various oligomerizations from monomer CH_3FBN_3 in the range of 200–800 K are compiled in Table 5. The values of ΔH in the processes are negative except for the process $1 \longrightarrow 2$ beyond 700 K, indicating that these oligomerization processes are exothermic. The ΔG at a given temperature is evaluated by the equation $\Delta G = \Delta H - T\Delta S$. The values of ΔG are all positive, which

Table 4: Thermodynamic properties for the most stable clusters $(CH_3FBN_3)_n$ $(n = 1-6)$ at different temperatures[a].

	T	200	298.2	400	500	600	700	800
1	$C^{\theta}_{p,m}$	77.73	96.48	113.47	127.30	138.62	147.95	155.71
	S^{θ}_{m}	305.18	339.77	370.57	397.42	421.66	443.75	464.03
	H^{θ}_{m}	11.30	19.87	30.58	42.65	55.96	70.30	85.50
2	$C^{\theta}_{p,m}$	161.34	206.04	243.12	271.97	295.00	313.71	329.19
	S^{θ}_{m}	409.57	482.65	548.58	606.05	657.75	704.68	747.61
	H^{θ}_{m}	19.88	38.00	60.94	86.75	115.14	145.61	177.78
3	$C^{\theta}_{p,m}$	242.25	312.13	369.54	413.90	449.12	477.62	501.12
	S^{θ}_{m}	509.21	619.50	719.58	807.00	885.70	957.14	1022.50
	H^{θ}_{m}	28.47	55.81	90.64	129.90	173.12	219.50	268.47
4	$C^{\theta}_{p,m}$	326.44	420.82	497.89	557.25	604.30	642.35	673.70
	S^{θ}_{m}	584.95	733.64	868.53	986.27	1092.19	1188.30	1276.18
	H^{θ}_{m}	37.13	74.00	120.94	173.82	231.98	294.38	360.23
5	$C^{\theta}_{p,m}$	411.59	530.37	627.05	701.33	760.11	807.59	846.71
	S^{θ}_{m}	686.62	874.08	1044.02	1192.26	1325.52	1446.38	1556.85
	H^{θ}_{m}	46.56	93.03	152.18	218.74	291.93	370.39	453.17
6	$C^{\theta}_{p,m}$	496.46	639.39	755.59	844.78	915.34	972.33	1019.26
	S^{θ}_{m}	788.60	1014.65	1219.48	1398.06	1558.56	1704.09	1837.08
	H^{θ}_{m}	55.96	111.99	183.27	263.47	351.61	446.09	545.74

[a]Units: T (K), $C^{\theta}_{p,m}$ (J·mol^{-1}·K^{-1}), S^{θ}_{m} (J·mol^{-1} K^{-1}), and H^{θ}_{m} (kJ·mol^{-1}).

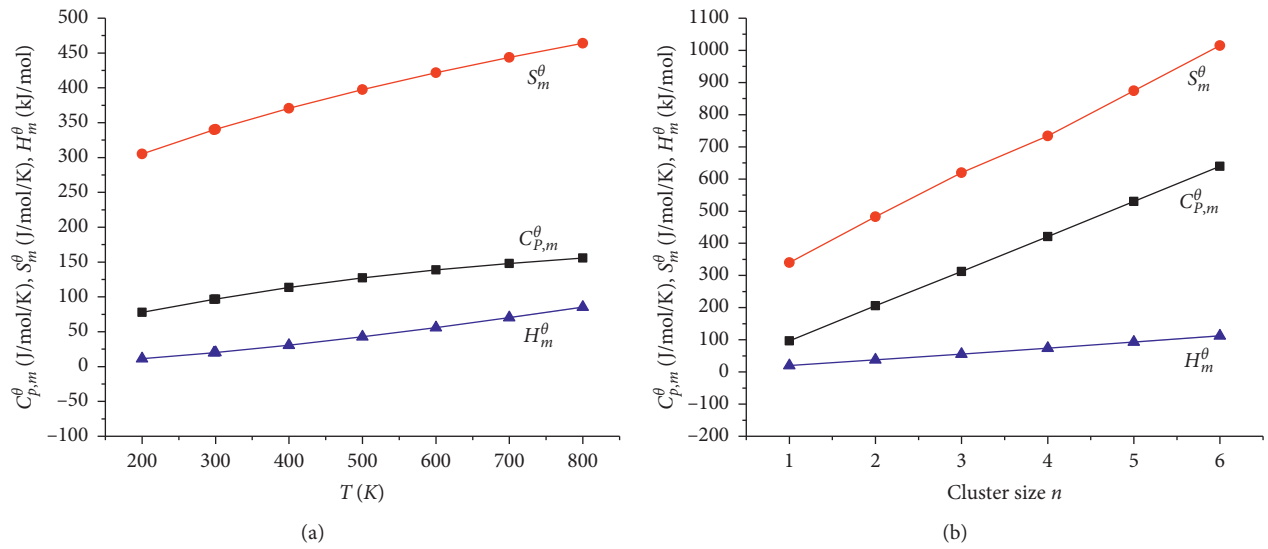

Figure 4: Variations of the thermodynamic functions ($C^{\theta}_{p,m}$, S^{θ}_{m}, and H^{θ}_{m}) with the temperature (T) (a) for the monomer CH_3FBN_3 and the cluster size n (b) and for the asymmetric clusters $(CH_3FBN_3)_n$ $(n = 1–6)$.

reveals the oligomerizations cannot occur spontaneously in the range of 200–800 K. There are no experimentally thermodynamic data available for the asymmetric clusters $(CH_3FBN_3)_n$ $(n = 1-6)$, so the calculated thermodynamic functions and the obtained relationships of them with the temperature and cluster size n may help the experiment to further study the physical, chemical, and energetic properties of the asymmetric clusters $(CH_3FBN_3)_n$ $(n = 1-6)$ or other asymmetric boron azides.

3.5. Aromatic Properties. Here, the aromaticity of the studied systems will be discussed. Because our systems are nonplanar, it is not suitable to use the criterion of nucleus-independent chemical shift (NICS) [30]. In order to find out whether a large π bond exists in our studied system, we use the newly proposed localized orbital locator (LOL)-π method [31] that can be used for studying nonplanar system to study the π bonds of our systems. The LOL-π is analyzed and visualized with the Multiwfn [32]. From Figure 5, there

Table 5: Enthalpy change and Gibbs free energy change of oligomerization at different temperatures[a].

	T	200	298.2	400	500	600	700	800
2(1) ⟶ (2)	ΔH	−7.22	−6.24	−4.72	−3.05	−1.28	0.51	2.28
	ΔG	32.94	52.45	72.30	91.35	110.06	128.48	146.64
3(1) ⟶ (3)	ΔH	−43.70	−42.07	−39.37	−36.32	−33.03	−29.67	−26.30
	ΔG	37.57	77.11	117.48	156.31	194.54	232.21	269.37
4(1) ⟶ (4)	ΔH	−61.34	−58.75	−54.65	−50.05	−45.13	−40.09	−35.04
	ΔG	65.81	127.69	190.85	251.66	311.54	370.60	428.91
5(1) ⟶ (5)	ΔH	−81.97	−78.35	−72.75	−66.54	−59.90	−53.14	−46.36
	ΔG	85.89	167.51	250.78	330.88	409.77	487.52	564.28
6(1) ⟶ (6)	ΔH	−98.66	−94.05	−87.03	−79.25	−70.97	−62.53	−54.08
	ΔG	109.84	211.20	314.55	413.98	511.87	608.36	703.60

[a]Units: T (K), ΔH (kJ·mol^{-1}), and ΔG (kJ·mol^{-1}).

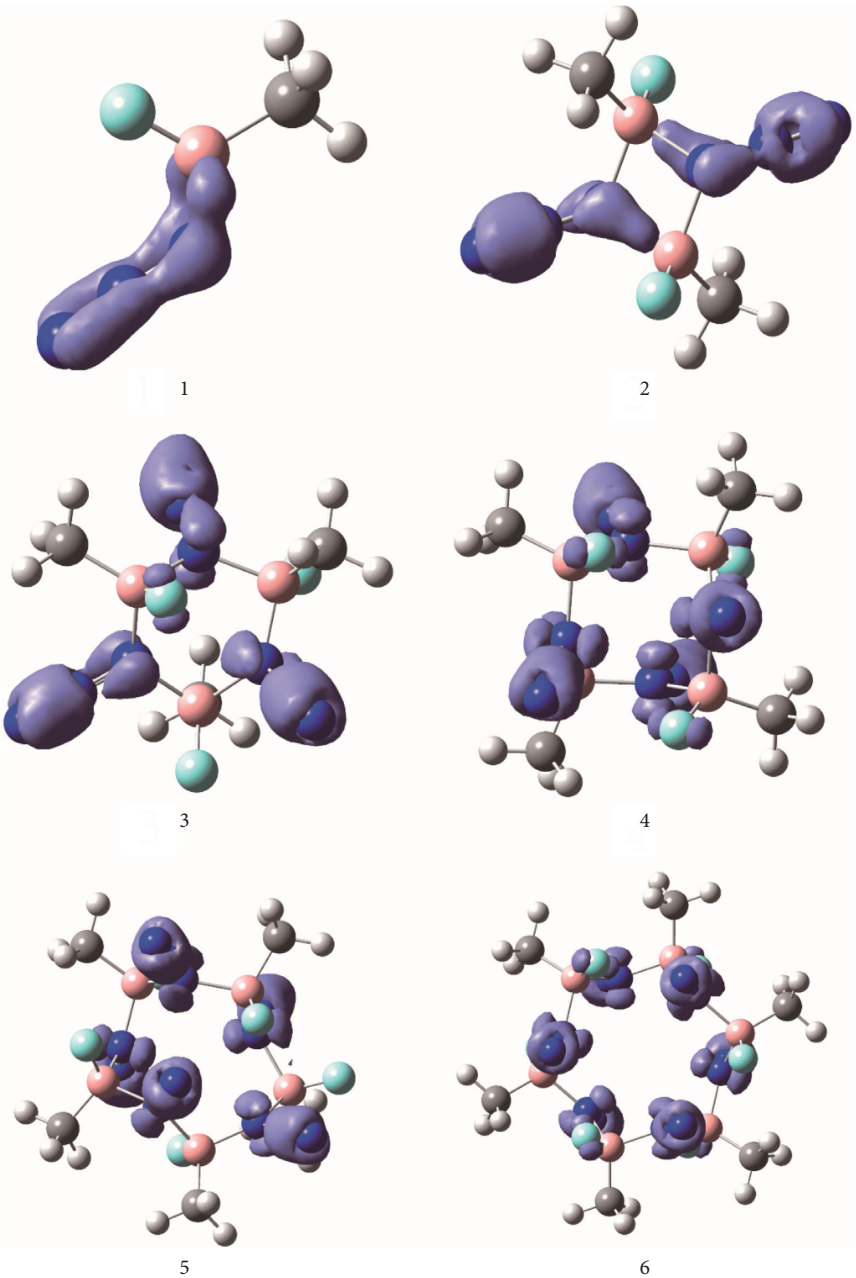

Figure 5: LOL-π isosurface of different systems with the isovalue of 0.4.

is π bond of NNNB in 1 and similar π bonds in 2-6. However, the π conjugation of 2–6 is not as good as that of 1. Meanwhile, Figure 5 also shows no large π bonds in all systems.

4. Conclusions

We have systematically studied the structure, relative stability, IR, and thermodynamic properties of the asymmetric clusters $(CH_3FBN_3)_n$ $(n = 1 - 6)$ at the DFT-B3LYP/6-31G*. The B and N_α atoms tend to bond together in clusters $(CH_3FBN_3)_n$ $(n = 2 - 6)$. The variation trend of geometrical parameters shows N_2 (N_β–N_γ), -CH_3, and F^- groups are easily eliminated and BN material is yielded. The calculated $\Delta_2 E$ of the asymmetric clusters (CH$_3$FBN3) n $(n = 1 - 6)$ exhibits a pronounced odd-even alternation phenomenon with cluster size n increasing, indicating that the cluster at $n = 3$ is more stable than other clusters. From monomer $(n = 1)$ to clusters $(n = 2 - 6)$, the N_3 asymmetric stretching vibration presents blue-shifted trend while the N_3 symmetric stretching vibration and –CH_3 stretching vibration are red-shifted. The thermodynamic functions ($C^\theta_{p,m}$, S^θ_m, and H^θ_m) of clusters $(CH_3FBN_3)_n$ $(n = 1 - 6)$ show linear increase with the augment of both temperature T and cluster size n of clusters. Judged by the enthalpies in the range of 298.2–600 K, the calculated thermodynamic properties demonstrate that the formation of clusters $(CH_3FBN_3)_n$ $(n = 2 - 6)$ from the monomer is thermodynamically favorable; however, the formation cannot occur spontaneously.

Data Availability

The data used to support the findings of this study are available from the corresponding author upon request.

Conflicts of Interest

The authors declare that there are no conflicts of interest regarding the publication of this paper.

Authors' Contributions

Qi-Ying Xia conceptualized the study and was responsible for project administration; Deng-Xue Ma, Yao-Yao Wei, and Yun-Zhi Li were involved in data curation; Guo-Kui Liu was involved in resource management; Deng-Xue Ma and Yao-Yao Wei wrote the original draft; and Qi-Ying Xia and Guo-Kui Liu wrote and edited the manuscript. Deng-Xue Ma and Yao-Yao Wei contributed equally to the work.

Acknowledgments

This work was supported by the Natural Science Foundation of Shandong Province (grant no. ZR2017LB011) and the Undergraduate Education Reform Project of Shandong Province (grant no. Z2018S006).

References

[1] R. L. Mulinax, G. S. Okin, and R. D. Coombe, "Gas phase synthesis, structure, and dissociation of boron triazide," *The Journal of Physical Chemistry*, vol. 99, no. 17, pp. 6294–6300, 1995.

[2] E. Wiberg and H. Michaud, "Notizen: zur kenntnis eines methylaluminiumdiazids $CH_3Al(N_3)2$," *Zeitschrift für Naturforschung B*, vol. 9, no. 7, p. 497, 1954.

[3] P. I. Paetzold, "Beiträge zur chemie der bor-azide. i. zur kenntnis von dichlorborazid," *Zeitschrift für Anorganische und Allgemeine Chemie*, vol. 326, no. 1-2, pp. 47–52, 1963.

[4] U. Müller, "Die kristall-und molekularstruktur von bordichloridazid $(BCl_2N_3)_3$," *Zeitschrift für Anorganische und Allgemeine Chemie*, vol. 382, no. 2, pp. 110–122, 1971.

[5] N. Wiberg, W.-Ch. Joo, and K. H. Schmid, "Uber einige azide des berylliums, magnesiums, bors und aluminiums (zur reaktion von silylaziden mit elementhalogeniden)," *Zeitschrift für Anorganische und Allgemeine Chemie*, vol. 394, no. 1-2, pp. 197–208, 1972.

[6] K. Dehnicke and N. Krüger, "Dijodo- und dibrommetallazide X_2MN_3 von aluminium und gallium," *Zeitschrift für anorganische und allgemeine Chemie*, vol. 444, no. 1, pp. 71–76, 1978.

[7] P. I. Paetzold and H.-J. Hansen, "Beiträge zur chemie der borazide. VI. zur kenntnis von dimethylborazid und seinen aminaten," *Zeitschrift für Anorganische und Allgemeine Chemie*, vol. 345, no. 1-2, pp. 79–86, 1966.

[8] J. Müller, P. Paetzold, and R. Boese, "The reaction of decaborane with hydrazoic acid: a novel access to azaboranes," *Heteroatom Chemistry*, vol. 1, no. 6, pp. 461–465, 1990.

[9] P. I. Paetzold, P. P. Habereder, and R. Müllbauer, "Beiträge zur chemie der borazide VII. darstellung und eigenschaften von diorganylboraziden," *Journal of Organometallic Chemistry*, vol. 7, no. 1, pp. 45–50, 1967.

[10] P. I. Paetzold, P. P. Habereder, and R. Müllbauer, "Beiträge zur chemie der borazide VIII. Thermischer zerfall von diorganylboraziden," *Journal of Organometallic Chemistry*, vol. 7, no. 1, pp. 51–60, 1967.

[11] W. Fraenk, T. M. Klapötke, B. Krumm, and P. Mayer, "Bis(pentafluorophenyl)boron azide: synthesis and structural characterization of the first dimeric boron azide," *Chemical Communications*, vol. 8, no. 8, pp. 667-668, 2000.

[12] W. Fraenk, T. M. Klapötke, B. Krumm, H. Nöth, M. Suter, and M. Warchhold, "Oligomeric pentafluorophenylboron azides," *Journal of the Chemical Society, Dalton Transactions*, no. 24, pp. 4635–4638, 2000.

[13] W. Fraenk, T. Habereder, A. Hammerl et al., "Highly energetic tetraazidoborate anion and boron triazide adducts†," *Inorganic Chemistry*, vol. 40, no. 6, pp. 1334–1340, 2001.

[14] P. I. Paetzold, "Darstellung, eigenschaften und zerfall von boraziden," in *Anorganische Chemie. Fortschritte der Chemischen Forschung*, vol. 8/3, pp. 437–469, Springer, Berlin, Germany, 2006.

[15] P. I. Paetzold, M. Gayoso, and K. Dehnicke, "Darstellung, Eigenschaften und Schwingungsspektren der trimeren Bordihalogenidazide $(BCl_2N_3)3$ und $(BBr_2N_3)_3$," *Chemische Berichte*, vol. 98, no. 4, pp. 1173–1180, 1965.

[16] M. J. Travers and J. V. Gilbert, "UV absorption spectra of intermediates generated via photolysis of $B(N_3)_3$, $BCl(N_3)_2$, and $BCl_2(N_3)$ in low-temperature argon matrices," *The Journal of Physical Chemistry A*, vol. 104, no. 16, pp. 3780–3785, 2000.

[17] R. Hausser-Wallis, H. Oberhammer, W. Einholz, and P. O. Paetzold, "Gas-phase structures of dimethylboron azide and dimethylboron isocyanate. Electron diffraction and ab initio study," *Inorganic Chemistry*, vol. 29, no. 17, pp. 3286–3289, 1990.

[18] L. A. Johnson, S. A. Sturgis, I. A. Al-Jihad, B. Liu, and J. V. Gilbert, "Low-temperature matrix isolation and photolysis of BCl_2N_3: spectroscopic identification of the photolysis product ClBNCl," *The Journal of Physical Chemistry A*, vol. 103, no. 6, pp. 686–690, 1999.

[19] W. Fraenk and T. M. Klapötke, "Theoretical studies on the thermodynamic stability and trimerization of BF_2N_3," *Journal of Fluorine Chemistry*, vol. 111, no. 1, pp. 45–47, 2001.

[20] D. X. Ma, Q. Y. Xia, and C. Zhang, "Theoretical studies on structural feature and thermodynamic stability of F_2BN_3 oligomers," *Journal of Atomic and. Molecular. Physics*, vol. 26, no. 2, pp. 361–367, 2009.

[21] A. Wang, Z. Chen, D. Ma, and Q. Xia, "Search for the structures, stabilities, IR spectra, and thermodynamic properties of the asymmetric clusters $(HClBN_3)$ n $(n = 1 - 6)$," *Russian Journal of Physical Chemistry A*, vol. 90, no. 13, pp. 2541–2549, 2016.

[22] Q. Y. Xia, D. X. Ma, D. J. Li, B. H. Li, X. Q. Wang, and G. F. Ji, "The molecular designs and properties of asymmetric heterocycles $(HBrBN_3)$ n $(n = 1 - 4)$," *Journal of Structural Chemistry*, vol. 56, no. 8, pp. 1468–1473, 2015.

[23] J. Kouvetakis, J. McMurran, C. Steffek, T. L. Groy, and J. L. Hubbard, "Synthesis and structures of heterocyclic azidogallanes $[(CH_3)ClGaN_3]_4$ and $[(CH_3)BrGaN_3]_3$ en route to $[(CH_3)HGaN_3]_x$: an inorganic precursor to GaN," *Inorganic Chemistry*, vol. 39, pp. 3805–3809, 2000.

[24] J. Kouvetakis, J. McMurran, C. Steffek, T. L Groy, J. L. Hubbard, and L. Torrison, "Synthesis of new azidoalanes with heterocyclic molecular structure," *Main Group Metal Chemistry*, vol. 24, no. 2, pp. 77–84, 2001.

[25] A. D. Becke, "Density-functional thermochemistry. III. The role of exact exchange," *The Journal of Chemical Physics*, vol. 98, no. 7, pp. 5648–5652, 1993.

[26] C. Lee, W. Yang, and R. G. Parr, "Development of the Colle-Salvetti correlation-energy formula into a functional of the electron density," *Physical Review B*, vol. 37, no. 2, pp. 785–789, 1988.

[27] M. J. Frisch, G. W. Trucks, H. B. Schlegel et al., *Gaussian 09, Revision A.02*, Gaussian, Inc., Pittsburgh, PA, USA, 2009.

[28] A. P. Scott and L. Radom, "Harmonic vibrational frequencies: an evaluation of Hartree–Fock, Møller–Plesset, quadratic configuration interaction, density functional theory, and semiempirical scale factors," *The Journal of Physical Chemistry*, vol. 100, no. 41, pp. 16502–16513, 1996.

[29] E. Lieber, D. R. Levering, and L. Patterson, "Infrared absorption spectra of compounds of high nitrogen content," *Analytical Chemistry*, vol. 23, no. 11, pp. 1594–1604, 1951.

[30] G. V. Baryshnikov, B. F. Minaev, N. N. Karaush, and V. A. Minaeva, "Design of nanoscaled materials based on tetraoxa[8]circulene," *Physical Chemistry Chemical Physics*, vol. 16, no. 14, pp. 6555–6559, 2014.

[31] T. Lu and Q. Chen, "A simple method of identifying π orbitals for non-planar systems and a protocol of studying π electronic structure," *Theoretical Chemistry Accounts*, vol. 139, no. 2, p. 25, 2020.

[32] T. Lu and F. Chen, "Multiwfn: a multifunctional wavefunction analyzer," *Journal of Computational Chemistry*, vol. 33, no. 5, pp. 580–592, 2012.